AJNR

MR Imaging of Periventricular Leukomalacia in Childhood

Olof Flodmark, Brian Lupton, David Li, Gary K. Stimac, Elke H. Roland, Alan Hill, Michael F. Whitfield and Margaret G. Norman

AJNR Am J Neuroradiol 1989, 10 (1) 111-118
http://www.ajnr.org/content/10/1/111

MR Imaging of Periventricular Leukomalacia in Childhood

Olof Flodmark[1]
Brian Lupton[2]
David Li[1]
Gary K. Stimac[3]
Elke H. Roland[2]
Alan Hill[2]
Michael F. Whitfield[2]
Margaret G. Norman[4]

Eight children with clinical and radiologic abnormalities consistent with periventricular leukomalacia were investigated with MR imaging of the brain that employed both inversion-recovery and T2-weighted spin-echo imaging sequences. The more precise delineation of white and gray matter on inversion-recovery images as compared with CT allows a detailed demonstration of the anatomic features of periventricular leukomalacia; specifically, a reduced quantity of white matter in the periventricular region and centrum semiovale and, in more severe cases, cavitated infarcts that replace the immediate periventricular white matter. The T2-weighted spin-echo and short inversion time inversion-recovery images demonstrated abnormally increased signal in white matter that appeared normal on CT scans and only minimally abnormal on conventional inversion-recovery images. These abnormalities most probably represent white matter gliosis that extends beyond the immediate periventricular regions.

MR recognition of cerebral white matter abnormalities associated with periventricular leukomalacia may confirm the clinical suspicion of this diagnosis in children with spastic diplegia or quadriplegia.

Recent advances in perinatal care have improved the survival rate of premature infants, resulting in greater awareness of perinatal cerebral injury and neurologic sequelae. Cerebral injury may result from intraventricular hemorrhage, which occurs in 35–50% of premature infants [1, 2], and from hypoxic-ischemic cerebral insults [3–9]. Of these two principal mechanisms of injury, the hypoxic-ischemic parenchymal injury is considered to be most significant and is most commonly associated with long-term sequelae. In the preterm infant, hypoxic-ischemic insult often results in periventricular leukomalacia (PVL), a specific pattern of injury with infarctions in the periventricular brain tissue [10–12].

Although neurosonography may demonstrate lesions consistent with PVL during the first weeks of life [8, 13–18], the reliability of this technique in the diagnosis of PVL has recently been questioned [19]. The sensitivity and specificity of this imaging technique have yet to be established. No study exists in which findings on neonatal neurosonography have been correlated with clinical outcome in an unselected group of children who have been observed long enough to establish the true incidence of spastic diplegia/quadriplegia likely to have been caused by PVL. Although the clinical correlate between perinatal injury and subsequent motor handicap may be quite clear in prematurely born children with a severe motor handicap, it is not uncommon that mild or moderate forms of spastic diplegia remain undiagnosed during the first 6 to 8 months of life, thus making the perinatal cause of the handicap less obvious. This may be particularly true if neurosonography during the neonatal period was reported as normal or if the injury happened during fetal life. The availability of MR is increasing, and it is quite likely that MR will be the preferred imaging method in the investigation of such a child, thus making it important for the neuroradiologist to recognize the changes of PVL as they appear on MR, even in older children and in the absence of a typical history.

This article appears in the January/February 1989 issue of *AJNR* and the March 1989 isue of *AJR*.

Received January 27, 1988; accepted after revision May 24, 1988.

Presented in part at the annual meeting of the American Society of Neuroradiology, New York, May 1987.

[1] Department of Radiology, University of British Columbia Children's Hospital, 4480 Oak St., Vancouver, B.C., Canada V6H 3V4. Address reprint requests to O. Flodmark.

[2] Department of Pediatrics, University of British Columbia Children's Hospital, Vancouver, B.C., Canada V6H 3V4.

[3] First Hill Diagnostic Center, Seattle, WA 98104.

[4] Department of Pathology, University of British Columbia Children's Hospital, Vancouver, B.C., Canada V6H 3V4.

***AJNR* 10:111–118, January/February 1989**
0195–6108/89/1001–0111

The purpose of this study is to describe the abnormalities observed on MR in children with the confirmed diagnosis of PVL.

Materials and Methods

The study population comprised eight children selected according to the following criteria: (1) motor abnormalities consistent with PVL, that is, spastic diplegia or quadriplegia; (2) gestational age less than 35 weeks; and (3) characteristic abnormalities of PVL on CT scans during late infancy. Two of the eight children had had intraventricular hemorrhage associated with intraparenchymal hemorrhage in the neonatal period. The patients were studied at a mean age of 5 years (range, 1–13 years).

MR imaging was performed on superconducting and, in one case, resistive 0.15-T systems.* All scans were obtained by using a contiguous 10-mm multislice technique. Both inversion recovery (IR) and spin-echo (SE) sequences were used to obtain images predominantly

* Picker International, Highland Heights, OH.

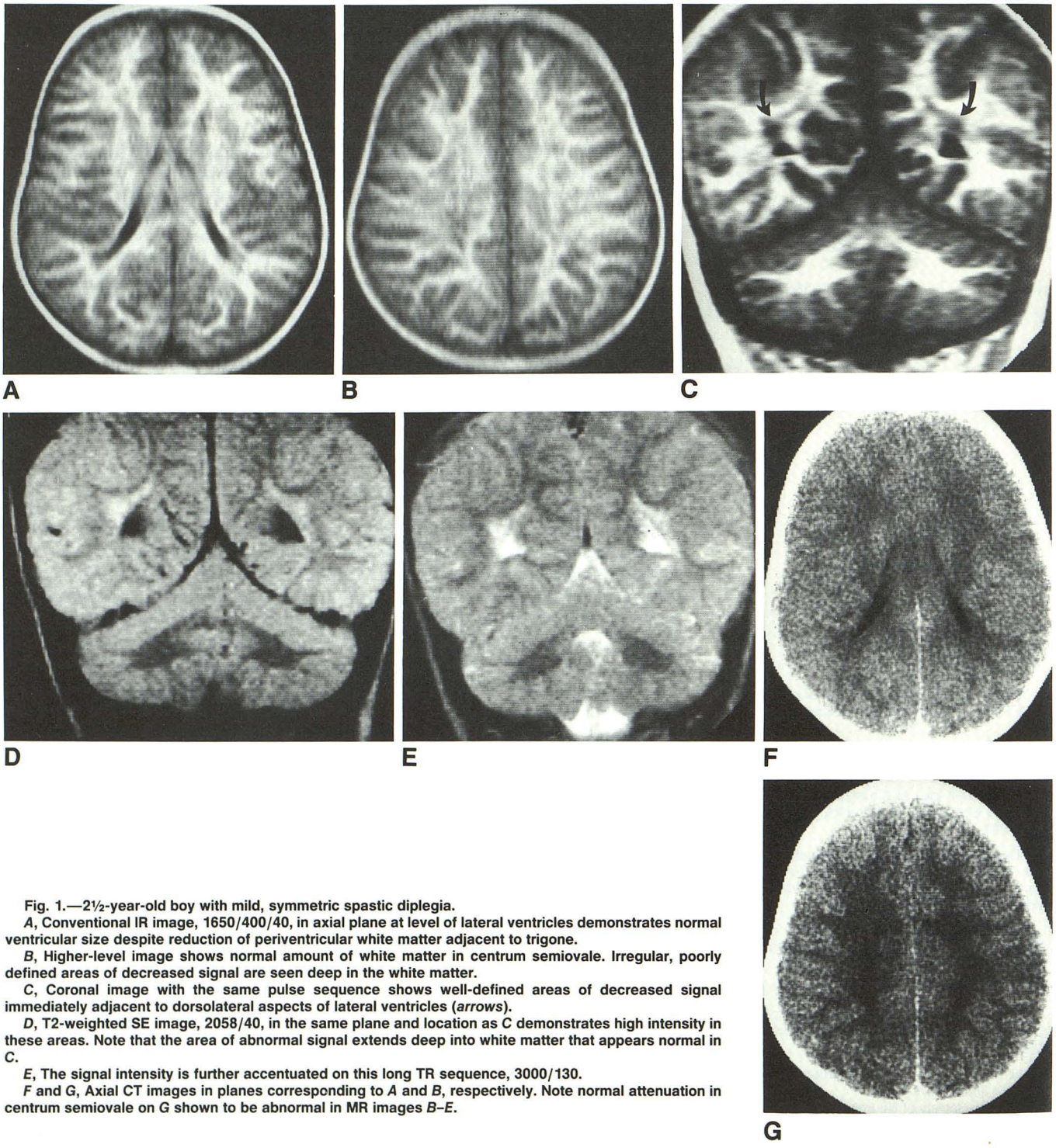

Fig. 1.—2½-year-old boy with mild, symmetric spastic diplegia.

***A*, Conventional IR image, 1650/400/40, in axial plane at level of lateral ventricles demonstrates normal ventricular size despite reduction of periventricular white matter adjacent to trigone.**

***B*, Higher-level image shows normal amount of white matter in centrum semiovale. Irregular, poorly defined areas of decreased signal are seen deep in the white matter.**

***C*, Coronal image with the same pulse sequence shows well-defined areas of decreased signal immediately adjacent to dorsolateral aspects of lateral ventricles (*arrows*).**

***D*, T2-weighted SE image, 2058/40, in the same plane and location as *C* demonstrates high intensity in these areas. Note that the area of abnormal signal extends deep into white matter that appears normal in *C*.**

***E*, The signal intensity is further accentuated on this long TR sequence, 3000/130.**

***F* and *G*, Axial CT images in planes corresponding to *A* and *B*, respectively. Note normal attenuation in centrum semiovale on *G* shown to be abnormal in MR images *B–E*.**

in the coronal planes but also in transaxial sections. Seven of the patients were scanned with conventional (long TI) IR sequences using the parameters of 1650/400/40/4 (TR/TI/TE/excitations) or 2450/400/40. Dual-echo coronal T2-weighted SE sequences, 2058/40, 120/2 (TR/first-echo TE, second-echo TE/excitations) or 2450/40, 120/2, were obtained in six patients, and one patient was examined with a multiple-echo long TR sequence (3000/26, 52, 104, 130, 156). Two patients were scanned with short TI IR (STIR) using 1183/100/40 or 1400/100/40. Single-echo T1-weighted SE sequences, 600/22, and T2-weighted SE sequences, 2000/60, were performed in an additional patient. Sedation was used as required (oral chloralhydrate 50 mg/kg). The MR examinations were approved by the Ethics Committee at the University of British Columbia and informed consent was obtained from the parents.

CT scans were performed with a GE CT/T 8800 scanner. Thin sections (5 mm) were obtained of the level of the lateral ventricles and viewed with a narrow window-width (60 H).

Results

Abnormalities on conventional IR scans were similar to those described previously on CT [20] and MR [21, 22]. The principal abnormality was reduction in the amount of periventricular white matter. With mild radiologic abnormality (two cases), this reduction of white matter, seen on both axial and coronal IR scans, was limited to the peritrigonal region. These patients had no or limited reduction of white matter in the centrum semiovale and the ventricular size was normal. As a consequence of this white matter loss, prominent sulci were identified adjacent to the trigone of the lateral ventricles and were proved on coronal IR scans to represent dilatation of the most posterior aspect of the sylvian fissure. Small, well defined lesions of reduced signal on IR scans and high intensity on T2-weighted SE and STIR scans were observed in the white matter immediately adjacent to the dorsolateral aspects of the lateral ventricles. This finding, best seen on coronal images, was present in all patients irrespective of age or severity of damage (Fig. 1).

With more severe radiologic involvement (five cases), there was evidence of reduction in the quantity of white matter in the centrum semiovale, indicating damage to the corona radiata. In addition there was more marked reduction of periventricular white matter. The deep portions of the sylvian fissures were prominent, and there was ventriculomegaly involving principally the occipital horns. The gray matter deep

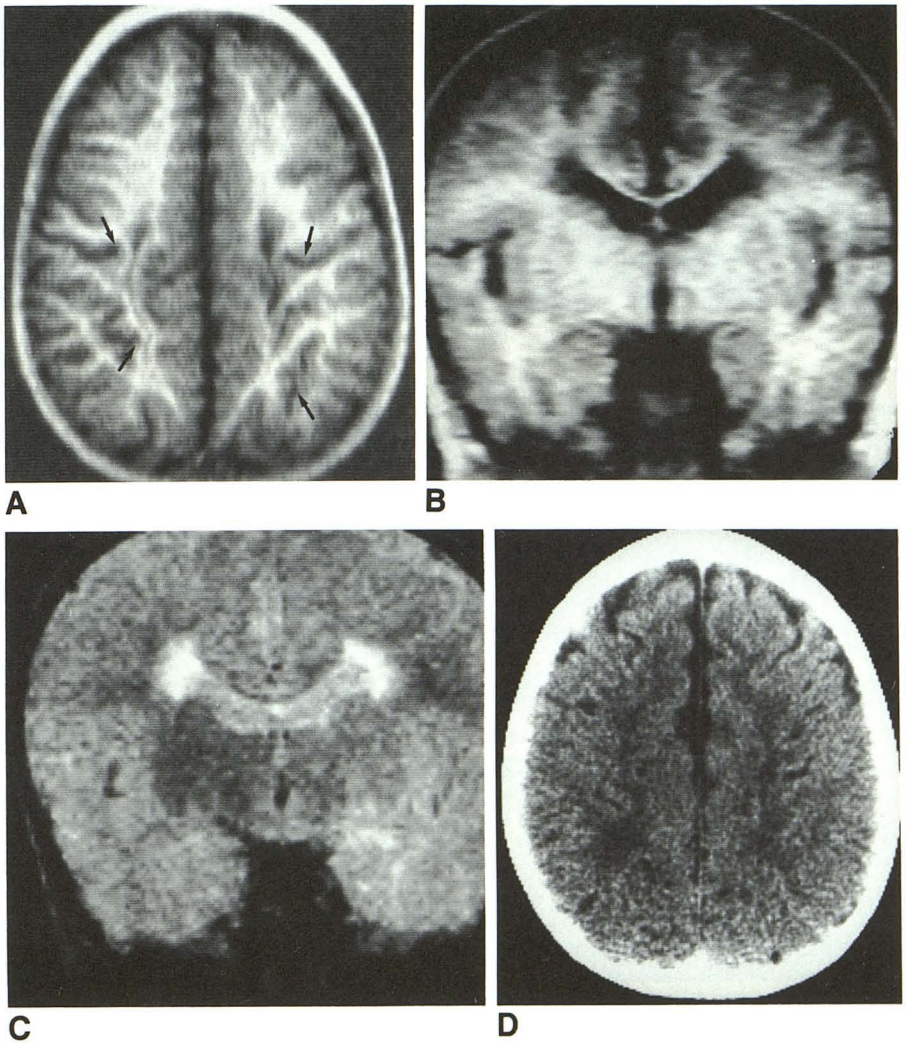

Fig. 2.—2½-year-old girl with moderately severe, symmetric spastic diplegia.

***A*, The end result from the periventricular infarction is demonstrated in this conventional IR image, 1650/400/40, in the axial plane, which shows a reduced amount of white matter in the centrum semiovale. Note the prominent, deep cortical sulci in close association with the ventricles (*arrows*).**

***B*, Conventional IR image, 1650/400/40, in the coronal plane shows the same finding as in Fig. 1C but in a more anterior location.**

***C*, Corresponding second-echo T2-weighted SE image, 2058/120, shows the high signal intensity within a more extensive area.**

***D*, Axial CT slice in a plane comparable to *A*. Note reduced amount of white matter with prominence of some of the same sulci as in *A*.**

within the sylvian fissure directly abutted and indented the ventricular wall or was separated from the ependyma by a minimal amount of white matter, resulting in an irregular ventricular outline and dilatation of the trigone (Figs. 2–5). The trigonal dilatation was most prominent in patients with profound cortical visual impairment (Fig. 3). More anterior coronal images demonstrated small, discrete areas of decreased signal in periventricular regions adjacent to the angles of the lateral ventricles. These lesions were visualized better on coronal than on axial MR images (Fig. 2).

One patient with PVL was severely affected clinically and had almost complete absence of white matter as shown on IR images. The periventricular white matter was replaced by cysts, some of which had been incorporated into the lateral ventricles, producing marked ventriculomegaly. As in the less severely affected patients with more moderate damage, the ventricular outline was irregular. Minimal amounts of white matter remained in the centrum semiovale. The gray matter deep within the sylvian fissure and the parietal lobes abutted the ventricles directly (Fig. 4).

Although the structural abnormalities on conventional IR images corresponded closely to those observed on CT scans [20], MR scans, particularly in the coronal plane, provided better anatomic resolution. The areas of decreased signal at the superior lateral margins of the lateral ventricles in patients with mild or moderate abnormalities had no correlate on CT scans, which demonstrated normal attenuation of white matter in these regions (Fig. 5).

Abnormally increased signal arising from white matter was observed on T2-weighted SE images in six of the seven patients with mild or moderate PVL. The increased signal corresponded in part to the areas of low signal on IR images but extended beyond the periventricular white matter. This increased white matter signal was observed principally in the

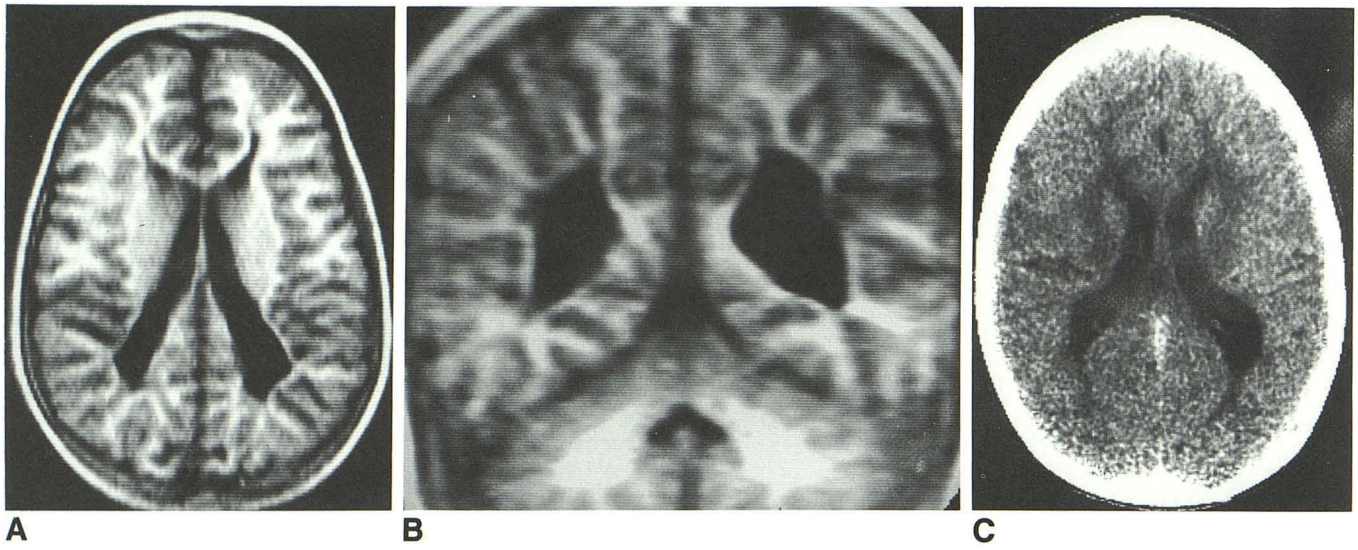

Fig. 3.—*A*, Conventional IR image, 1650/400/40, in the axial plane of 6-year-old girl who had only mild spastic diplegia but was cortically blind. Note the disproportionate dilatation of the occipital horns with almost complete absence of white matter in the occipital lobes.
***B*, Coronal image, 2450/400/40, shows how the cortical sulci extend down to the ventricular wall with very little remaining white matter.**
***C*, Axial CT scan in a plane similar to *A* shows that the appearance of the ventricles and periventricular white matter correlates very well with the findings in *A*.**

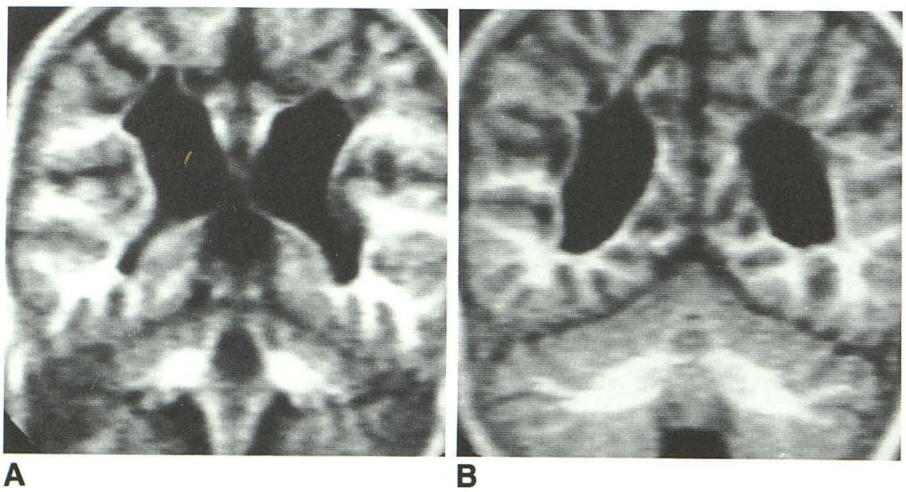

Fig. 4.—*A* and *B*, Conventional IR images, 2450/400/40, of 5-year-old boy with severe quadriplegia, which was more severe on the left side of the body, and cortical blindness show an almost complete absence of all periventricular white matter and subsequent marked ventricular dilatation. Note the larger right ventricle with a more irregular dorsolateral aspect, indicating more severe involvement on the right side.

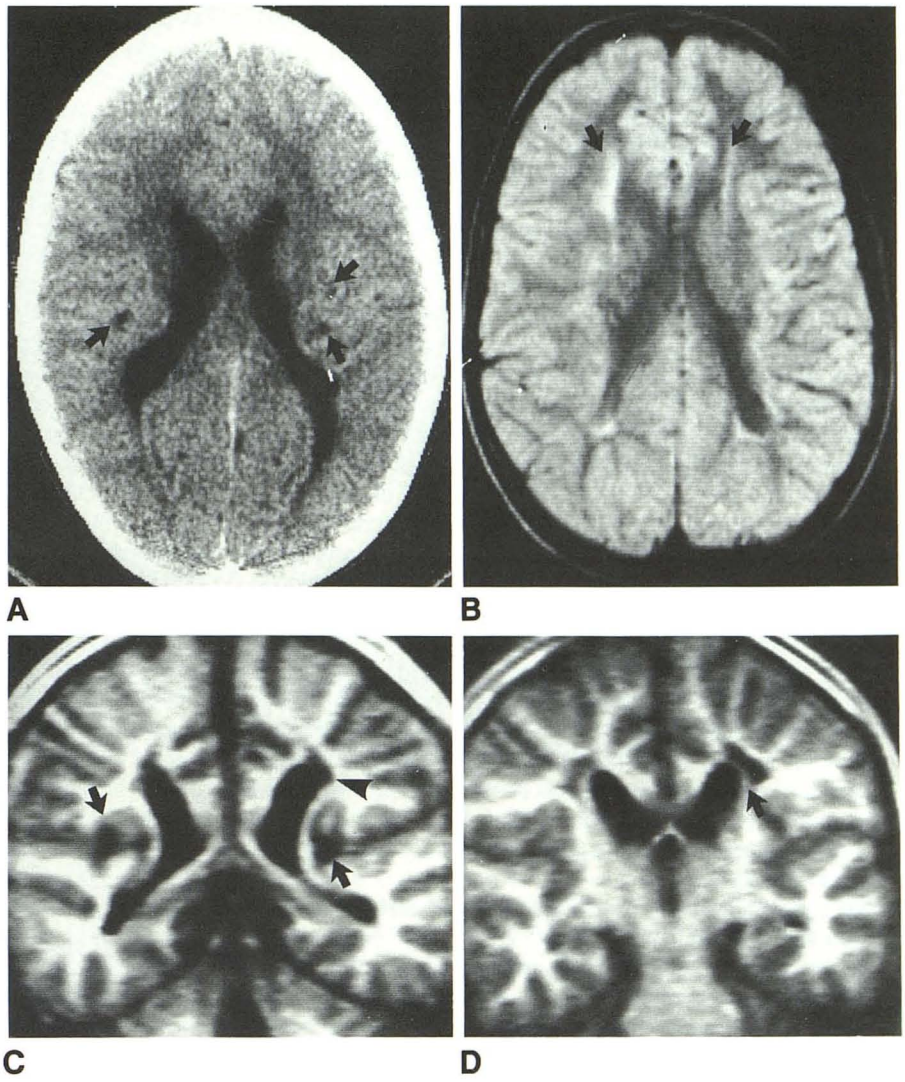

Fig. 5.—*A*, CT scan of 9-year-old boy with moderate to severe quadriplegia shows virtually complete absence of peritrigonal white matter, with less severe loss of white matter anteriorly. The ventricles are moderately dilated. Note superficial "cystic" structures (*arrows*) in cortical tissue, and normal appearance of white matter deep in the frontal lobes.

***B*, Corresponding T2-weighted SE image, 2450/40, shows abnormal signal intensity in frontal white matter (*arrows*), tissue that had a normal CT appearance in *A*.**

***C*, Conventional IR image, 1650/400/40, in the coronal plane demonstrates clearly that the "cystic" structures in the cortex represent widening of the deep parts of the sylvian fissure (*arrows*). Note the square shape of the dorsolateral aspects of the left ventricle (*arrowhead*), indicating that cavitated periventricular infarcts have become incorporated into the ventricle. The injury is less prominent on the right side, where the ventricle has maintained a more normal shape and more periventricular white matter with normal signal intensity remains. The child had an asymmetric quadriplegia, which was more severe in the right leg and arm.**

***D*, A more anterior image in the same sequence shows a part of the periventricular cavitated infarct on the left side, which has maintained the thin wall separating it from the ventricle (*arrow*).**

occipital lobes and extended into regions that appeared normal on CT and conventional IR images. The signal characteristics of these lesions differed from that of CSF by showing a high intensity on first-echo SE images. These lesions were also well shown by STIR because of the high tissue contrast with respect to normal white matter. White matter located more superficially (i.e., subcortically) and deep within the centrum semiovale demonstrated a normal appearance (Figs. 1 and 2).

In all cases, there was good correlation between clinical observations and the anatomic location of MR and CT abnormalities. In patients with asymmetric motor involvement, the MR and CT abnormalities corresponded to the clinical observations.

Discussion

Periventricular leukomalacia results from hypoxic-ischemic injury to watershed zones of arterial supply in the periventricular white matter of the immature brain [10–12, 23]. These watershed zones are most prominent in the posterior periventricular white matter at the trigone of the lateral ventricles and in white matter adjacent to the foramina of Monro [10–12]. Additional injury may result from parenchymal hemorrhage in association with ischemic lesions, a finding that has been reported in approximately 25% of cases in an autopsy study. This likely represents spontaneous hemorrhage into reperfused periventricular ischemic areas; that is, hemorrhagic infarction [23]. The anatomic location of PVL determines the characteristic neurologic sequelae observed in many survivors of low birth weight. Thus, lesions may affect either the geniculocalcarine tract and cause visual impairment or the corticospinal tracts in the corona radiata and damage the motor fibers, which control the function of lower limbs and trunk. Consequently, the classical neurologic sequelae of PVL include spastic diplegia or quadriplegia, and cortical blindness with relative preservation of cognitive functions, except in severe cases. In severe cases, the cerebral injury is more diffuse and results in multiple neurologic handicaps [10, 11].

Histopathologically, periventricular leukomalacia begins as coagulation necrosis with subsequent macrophage activity

and cavitation [10]. The cavitated infarcts are located principally at the dorsolateral margins and at the trigone of the ventricles. The cysts may collapse, resulting in scarring with gliosis associated with significant reduction in the quantity of white matter in periventricular regions and in the centrum semiovale. With severe PVL, the cavities may replace most of the periventricular white matter. The ependymal separation between the ventricles and the cavitated infarcts may completely or partially break down, and the cavitated infarcts become incorporated into the ventricles. This process explains in part the characteristic ventriculomegaly with irregular ventricular outline.

Radiologic imaging techniques may play an important role in the confirmation of the diagnosis of PVL by demonstrating evidence of injury to periventricular white matter. Although neurosonography is useful, its limitations are probably significant but not well studied [8, 14–19]. CT is of less value during the neonatal period [2, 24] but can demonstrate pathognomonic abnormalities of PVL in later infancy and childhood [15, 17, 20]. The clinical diagnosis of PVL in such a child may be confirmed by CT scanning, which demonstrates specific diagnostic features of PVL, including (1) ventriculomegaly with irregular outline of body and trigone of lateral ventricles; (2) reduced amounts of periventricular white matter at the trigone and, in more severe cases, the entire centrum semiovale; and (3) deep and prominent sulci with subcortical gray matter abutting the ventricles directly without interposed white matter [20]. These abnormalities were identified on all CT scans performed in close temporal relationship to the MR scans in our study.

MR imaging has been used in a limited fashion for the study of neonatal cerebral injury [8, 21, 25–30]. Although limited data are available regarding the appearance of PVL on MR during the neonatal period [22], the role of MR for the diagnosis of PVL in early infancy has not been defined clearly. Furthermore, there are no published reports describing the appearance of this lesion on MR imaging in older children. MR studies of infants with sonographic evidence of PVL during the neonatal period showed decreased signal in periventricular white matter on conventional IR images [27, 31]. Serial MR examinations showed development of an irregular outline of dilated lateral ventricles and delayed myelination. The decreased intensity of periventricular signal relates most probably to loss of white matter associated with infarction and cyst formation. The delayed myelination reported by others [21, 31] relates to ischemic destruction of unmyelinated axons in the immature brain and thus to reduced formation of myelin. The location of these abnormalities in early infancy correlated well with the distribution of cysts, reduced white matter, and the resultant prominence of deep portions of cortical sulci and sylvian fissures during later childhood in our patients. Although delayed myelination of the periventricular brain tissue may be observed during early infancy, it is unlikely to persist into later childhood. Thus, the abnormalities observed in older children most probably represent permanent loss of tissue with gliosis.

Several studies have reported more superficial cystic cavities located at some distance from the ventricles in gray matter [26, 27, 31]. In our patients, conventional IR images in the coronal plane demonstrate clearly that these "cystic" structures represent widened sulci deep within the sylvian fissures. Loss of periventriuclar white matter results in widening of sulci such that they become visible on axial CT or MR scans. Owing to the effect of volume averaging, the continuity of these sulci with the sylvian fissure may not be immediately apparent in the axial plane (Fig. 5).

The areas of high intensity in white matter extending superficially beyond the periventricular region seen well on T2-weighted SE and STIR images (Fig. 6) but not on CT scans, most probably represent areas of gliosis with scarring extending further into central white matter within gyri (Fig. 7). Although described by pathologists [10, 11], these lesions, characteristic of PVL, have not previously been recognized by any radiologic imaging technique. These changes are probably similar in pathology to areas of gliosis seen in patients with multiple sclerosis, infarcts particularly those in deep white matter (Binswanger disease), and in the late stages following head injury [32]. In all these situations the abnormal areas have a higher signal than that of CSF on moderately T2-weighted SE imaging sequences (2000/40). Thus, these lesions can be differentiated from cavitated infarcts that are more similar to CSF in their signal characteristics. Such cysts were seen in patients with moderate and severe injury in whom the immediate periventricular white matter was replaced by cysts. In this study, the abnormalities on MR scans were located most frequently in the posterior periventricular region at the trigone of the lateral ventricles. This corresponds to the location of PVL documented previously by autopsy studies [12].

A variety of imaging sequences were employed in the evaluation of our patients. Images in the coronal plane were most effective both for identifying structural abnormalities and for determining the location of parenchymal disease. This advantage was due mainly to the orientation of the coronal plane perpendicular to the long axes of the sylvian fissure and the lateral ventricles. Structural abnormalities, including the deep sulci, ventricular enlargement, and irregular ventricular margins, were best shown on the conventional (long TI) IR and T1-weighted SE sequences because they showed the CSF as low intensity in contrast to the adjacent brain. The periventricular white matter abnormalities were best shown on T2-weighted SE and STIR images because of the high contrast between the lesions and the surrounding intact white matter. These lesions were not identified on T1-weighted SE images at low field strength (0.15 T) because of the similarity of gray matter, white matter, and most abnormalities characterized by increased water content. The lesions were demonstrated on the conventional IR scans but, because they appeared as low density, were less obvious than on the T2-weighted SE and STIR images. The size of these abnormalities was underestimated on the conventional IR scans. In our experience, it appears that an investigation of possible PVL should include coronal sequences that provide high anatomic detail, such as conventional IR or T1-weighted SE, and a sequence that provides high tissue contrast, such as T2-weighted SE or STIR. The shorter acquisition time involved in a STIR sequence may prove advantageous in a pediatric population. The use of thinner sections, 5 mm or thinner,

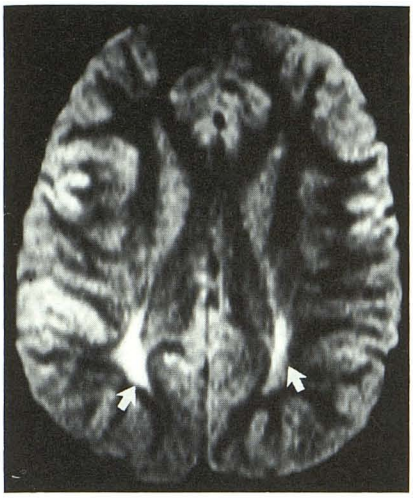

Fig. 6.—Axial STIR image, 1400/100/40, provides less anatomic detail than some T2-weighted SE images but shows well the abnormal signal (*arrows*) in the periventricular white matter.

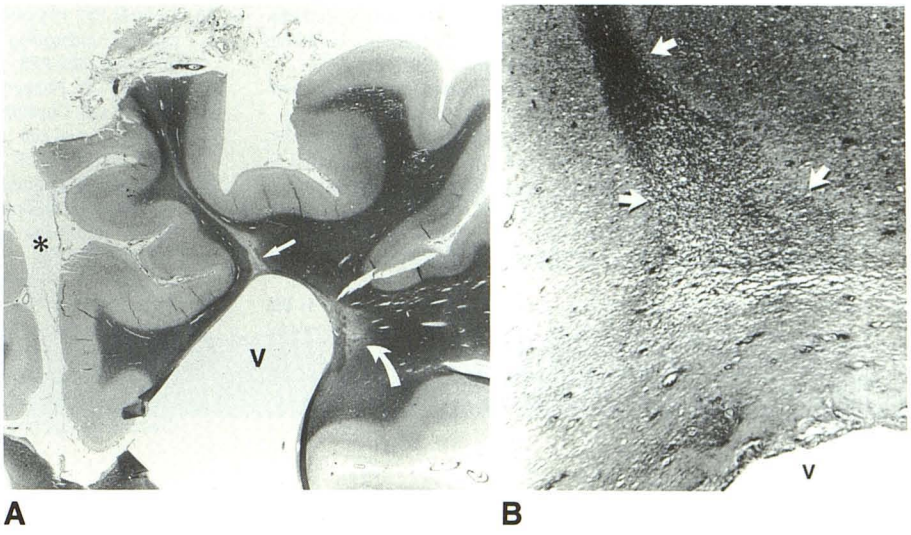

Fig. 7.—Histologic sections of 19-year-old man, not part of this study, who was a first-born twin. Birth was at 30 weeks gestation with a difficult delivery. He had severe spastic quadriplegia, abnormal posture, and he was cortically blind. He could speak one or two words and could not respond to command. His brain weighed 1220 g (normal, 1500 g).

A, Whole tissue mount shows an unmyelinated scar (*straight arrow*) extending from enlarged ventricle (V) into the postcentral gyrus. Another scar (*curved arrow*) with focal calcification is seen in the paraventricular white matter. The interhemispheric fissure (*asterisk*) is identified. (Luxol fast blue/cresyl violet stain, ×4)

B, This section shows another similar scar (*arrows*) stained for glial fibers. The lesion extends into the frontal lobe and represents gliosis. (V = ventricle.) (Holzer stain, ×50)

proved essential for the CT diagnosis of PVL [20]. A similar technique able to show even minimal amounts of disease in the periventricular white matter may prove as important in MR imaging. However, the limited field strength of our MR systems prevented us from using this technique.

ACKNOWLEDGMENTS

We thank J. Wada, J. E. Jan, and K. Farrell for allowing us to study their patients.

REFERENCES

1. Papile LA, Munsick-Bruno G, Schaefer A. Relationship of cerebral intraventricular hemorrhage and early childhood neurologic handicap. *J Pediatr* **1983**;103:273–277
2. Flodmark O, Fitz CR, Harwood-Nash DC. CT diagnosis and short-term prognosis of intracranial hemorrhage and hypoxic ischemic brain damage in neonates. *J Comput Assist Tomogr* **1980**;4:775–787
3. Dubowitz LMS, Dubowitz V, Palmer PG, Miller G, Fawer CL, Levene MI. Correlation of neurologic assessment in the preterm newborn infant with outcome at 1 year. *J Pediatr* **1984**;105:452–456
4. Fitzhardinge PM, Flodmark O, Fitz CR, Ashby S. The prognostic value of computed tomography of the brain in asphyxiated premature infants. *J Pediatr* **1982**;100:476–481
5. Flodmark O. Diagnosis by computed tomography of intracranial hemorrhage and hypoxic/ischemic brain damage in neonates (thesis). Karolinska Institute, Stockholm, Sweden, **1981**
6. Fawer CL, Levene MI, Dubowitz LMS. Intraventricular haemorrhage in a preterm neonate: discordance between clinical course and ultrasound scan. *Neuropediatrics* **1983**;14:242–244
7. Shankaran S, Slovis TL, Bedard MP, Poland RL. Sonographic classification of intracranial hemorrhage. A prognostic indicator of mortality, morbidity, and short-term neurologic outcome. *J Pediatr* **1982**;100:469–475
8. Dubowitz LMS, Bydder GM, Mushin J. Developmental sequence of periventricular leukomalacia: correlation of ultrasound, clinical, and nuclear magnetic resonance functions. *Arch Dis Child* **1985**;60:349–355
9. Bozynski MEA, Nelson MN, Matalon TAS, et al. Cavitary periventricular leukomalacia: incidence and short-term outcome in infants weighing < 1200 grams at birth. *Dev Med Child Neurol* **1985**;27:572–577
10. DeReuck J, Chatta AS, Richardson EP Jr. Pathogenesis and evolution of periventricular leukomalacia in infancy. *Arch Neurol* **1972**;27:229–236
11. Banker BQ, Larroche JC. Periventricular leukomalacia of infancy. *Arch Neurol* **1962**;7:386–410
12. Shuman RM, Selednik LJ. Periventricular leukomalacia: a one-year autopsy study. *Arch Neurol* **1980**;37:231–235
13. Weindling AM, Rochefort MJ, Calvert SA, Fok T-F, Wilkinson A. Development of cerebral palsy after ultrasonographic detection of periventricular cysts in the newborn. *Dev Med Child Neurol* **1985**;27:800–806
14. Bowerman RA, Donn SM, DiPeitro MA, D'Amato CJ, Hicks SP. Periventricular leukomalacia in the pre-term newborn infant: sonographic and clinical features. *Radiology* **1984**;151:383–388
15. Chow PP, Horgan JG, Taylor KJW. Neonatal periventricular leukomalacia: real-time sonographic diagnosis with CT correlation. *AJNR* **1985**; 6:383–388
16. Nwaesei CG, Pape KE, Martin DJ, Becker LE, Fitz CR. Periventricular infarction diagnosed by ultrasound: a postmortem correlation. *J Pediatr* **1984**;105:106–110
17. Schellinger D, Grant EG, Richardson JD. Cystic periventricular leukomalacia: sonographic and CT findings. *AJNR* **1984**;5:439–445
18. Szymonowicz W, Schafler K, Cussen LJ, Yu VYH. Ultrasound and necropsy study of periventricular haemorrhage in preterm infants. *Arch Dis Child* **1984**;59:637–642
19. Baarsma R, Laurini RN, Baerts W, Okken A. Reliability of sonography in non-hemorrhagic periventricular leukomalacia. *Pediatr Radiol* **1987**;17: 189–191
20. Flodmark O, Roland EH, Hill A, Whitfield MF. Periventricular leukomalacia: radiologic diagnosis. *Radiology* **1987**;162:119–124
21. Wilson DA, Steiner RE. Periventricular leukomalacia: evaluation with MR imaging. *Radiology* **1986**;160:507–511

22. De Vries LS, Connell JA, Dubowitz LMS, Oozeer RC, Dubowitz V, Pennock JM. Neurological, electrophysiological and MRI abnormalities in infants with extensive cystic leukomalacia. *Neuropediatrics* **1987**;18:61–66
23. Armstrong D, Norman MG. Periventricular leucomalacia in neonates: complications and sequelae. *Arch Dis Child* **1974**;49:367–375
24. Flodmark O, Becker LE, Harwood-Nash DC, Fitzhardinge PM, Fitz CR, Chuang SH. Correlation between computed tomography and autopsy in premature and full-term neonates that have suffered perinatal asphyxia. *Radiology* **1980**;137:93–103
25. Johnson MA, Pennock JM, Bydder GM, et al. Clinical NMR imaging of the brain in children: normal and neurologic disease. *AJNR* **1983**;4: 1013–1026
26. Dubowitz LMS, Bydder GM. Nuclear magnetic resonance imaging in the diagnosis and follow-up of neonatal cerebral injury. *Clin Perinatol* **1985**;12(1):243–260
27. Johnson MA, Pennock JM, Bydder GM, Dubowitz LMS, Thomas DJ, Young IR. Serial MR imaging in neonatal cerebral injury. *AJNR* **1987**;8: 83–92
28. McArdle CB, Nicholas DA, Richardson CJ, Amparo EG. Monitoring of the neonate undergoing MR imaging: technical considerations. *Radiology* **1986**;159:223–226
29. McArdle CB, Richardson CJ, Nicholas DA, Mirfakhraee M, Hayden CK, Amparo EG. Developmental features of the neonatal brain: MR imaging. Part I, gray-white matter differentiation and myelination. *Radiology* **1987**;162:223–229
30. McArdle CB, Richardson CJ, Nicholas DA, Mirfakhraee M, Hayden CK, Amparo EG. Developmental features of the neonatal brain: MR imaging. Part II, ventricular size and extracerebral space. *Radiology* **1987**;162: 230–234
31. McArdle CB, Richardson JC, Hayden CK, Nicholas DA, Amparo EG. Abnormalities of the neonatal brain: MR imaging. Part II, hypoxic-ischemic brain injury. *Radiology* **1987**;163:395–403
32. Bradley WG, Kortman KE. Magnetic resonance imaging of non-neoplastic central nervous system abnormalities. In: Mettler FA, Muroff LR, Kulkarni MV, eds. *Magnetic resonance imaging and spectroscopy,* New York: Churchill Livingstone, **1986**:15–41